Stepwise Structural Evolution of a DTS-F_2BT Oligomer and Influence of Structural Disorder on OFET and OPV Performance

Chi-Feng Huang,[a] Sin-Hong Huang,[a] Chou-Ting Hsieh,[a] Yi-Hsiang Chao,[a] Chia-Hua Li,[a] San-Lien Wu,[a] Yi-Fan Huang,[a] Chen-Yang Hong,[a] Chain-Shu Hsu,[a] Wei-Tsung Chuang,[b*] and Chien-Lung Wang[a*]

[a]Department of Applied Chemistry, National Chiao Tung University, 1001 Ta Hsueh Road Hsinchu, 30010, Taiwan

[b]National Synchrotron Radiation Research Center, 101 Hsin-Ann Road, Hsinchu Science Park, Hsinchu, 300, Taiwan

*E-mail: weitsung@nsrrc.org.tw kclwang @nctu.edu.tw

Supporting information

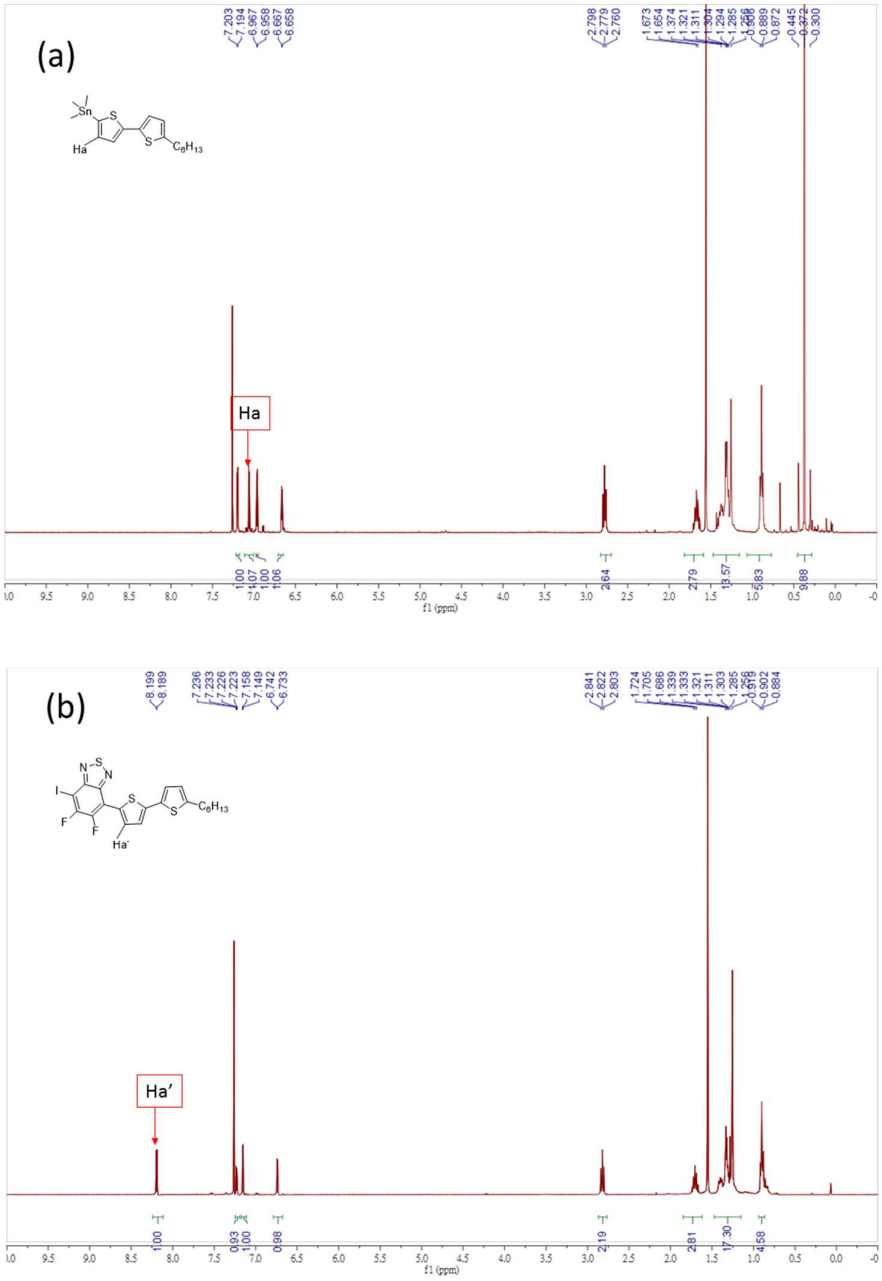

Figure S1. ^{1}H NMR spectra of (a) **2** and (b) **3**

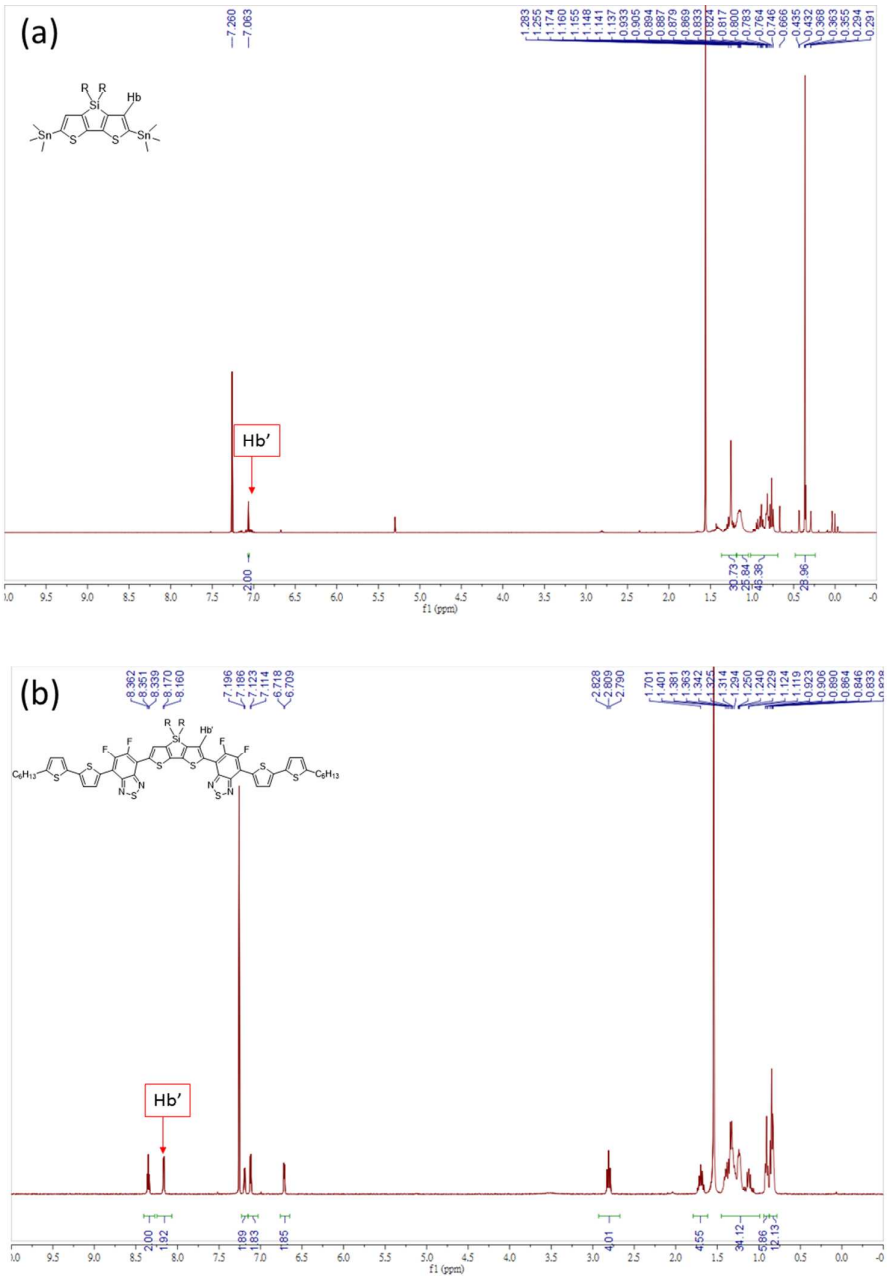

Figure S2. ^{1}H NMR spectra of (a) **4** and (b) DTS(F_2BT)$_2$

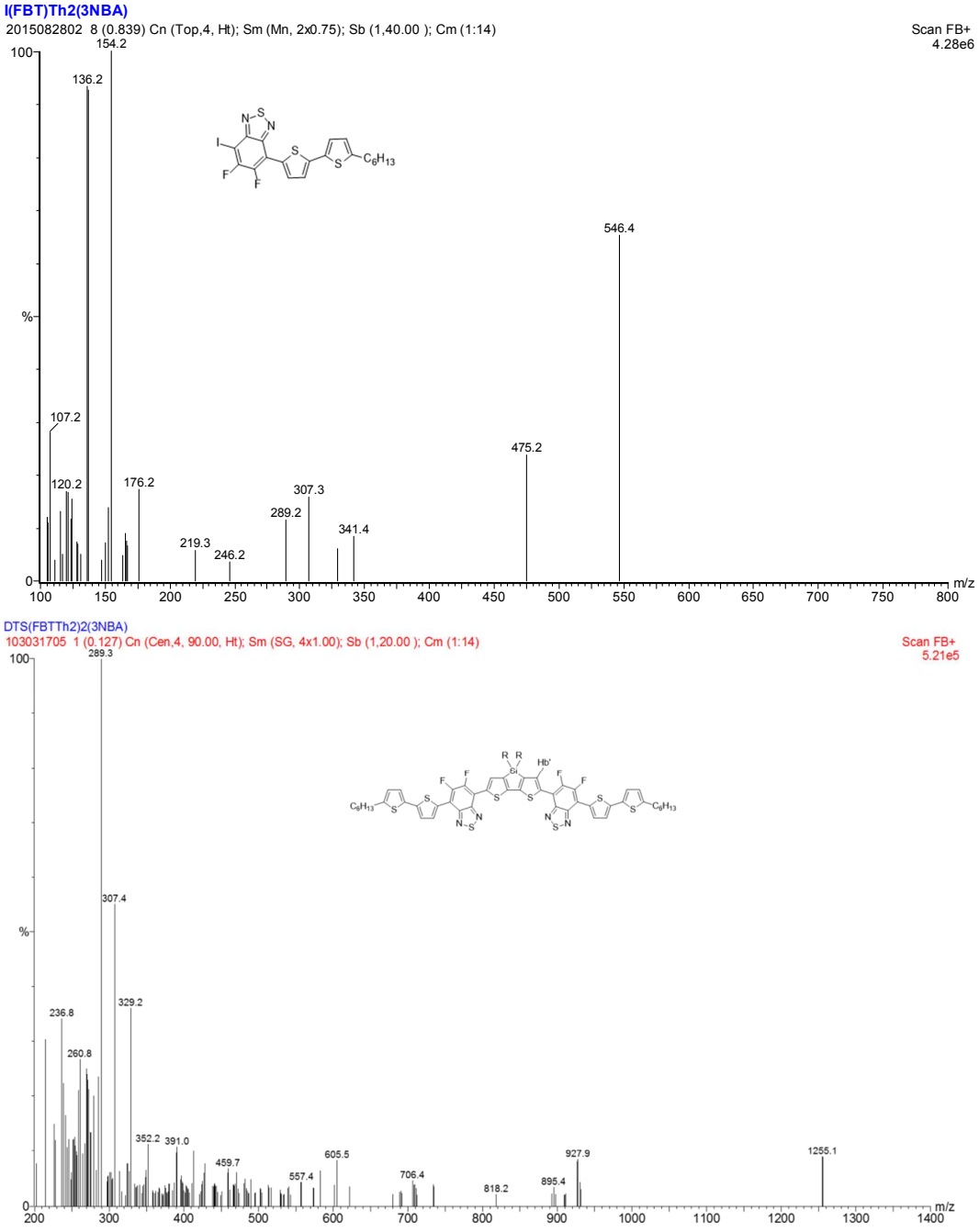

Figure S3. Mass spectra of (a) **3** and (b) DTS(F_2BT)$_2$.

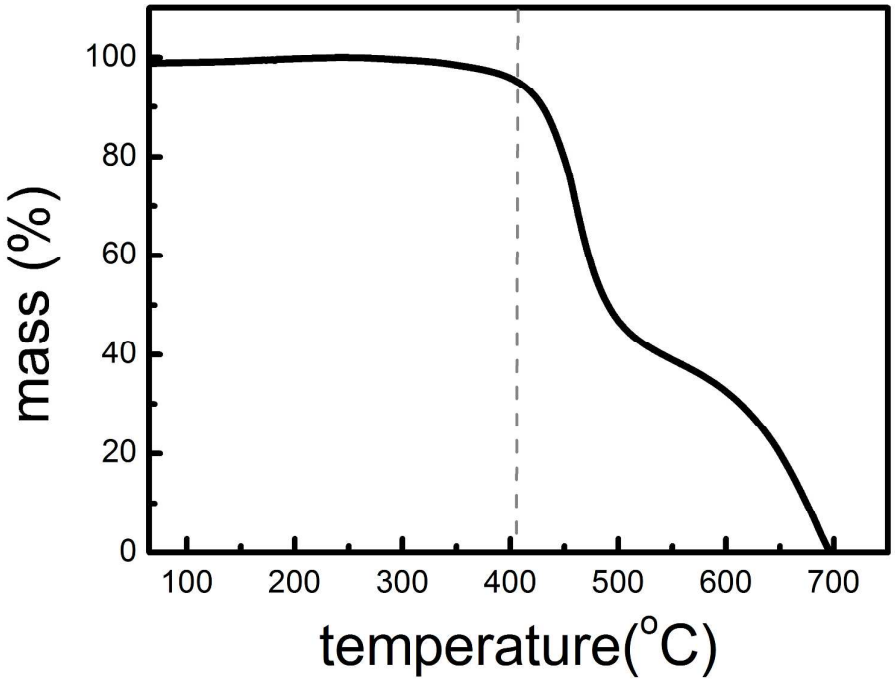

Figure S4. Thermogravimetric analysis of DTS(F_2BT)$_2$. The temperature of dissociation is 406 ° C.

Table S1. Crystallographic Parameters of DTS(F_2BT)$_2$ from GI-XRD

(*hkl*)	$d_{obs.}$ /nm	$d_{calc.}$ /nm	I_{exp}	ϕ	(*hkl*)	$d_{obs.}$ /nm	$d_{calc.}$ /nm	I_{exp}	ϕ
(200)	2.27	2.27	100	π	(101)	2.31	2.29	1.96	π
(400)	1.15	1.13	24.88	π	(201)	1.28	1.72	2.96	0
(600)	0.77	0.76	4.97	π	(301)	1.23	1.31	1.51	π
(110)	0.93	0.93	1.34	0	(102)	1.05	1.27	1.31	0
(210)	0.88	0.88	1.36	0	(202)	1.15	1.14	1.22	π
(310)	0.82	0.80	2.06	0	(302)	0.98	1.00	1.23	0
(510)	0.67	0.67	1.57	0	(402)	0.83	0.86	1.27	π
(720)	0.4	0.38	1.47	0	(502)	0.73	0.75	1.27	0
(120)	0.46	0.47	0.95	0	(602)	0.60	0.66	1.29	π
(020)	0.48	0.48	1.21	π	(702)	0.51	0.58	2.07	0
-	-	-	-	-	(703)	0.47	0.52	1.21	π
a = 4.54 nm; b = 0.96 nm; c = 2.65 nm									
$\alpha = \beta = \gamma = 90^o$									

Table S2. Crystallographic Parameters of DTS(F_2BT)$_2$ from 2D WAXD

(hkl) plane	Experimental *d*-spacing $d_{obs.}$ /nm	Theoretical *d*-spacing $d_{calc.}$ /nm
(200)	2.3	2.27
(400)	1.15	1.14
(600)	0.76	0.76
(020)	0.49	0.48
(11 1 0)	0.43	0.38
(002)	1.36	1.33
(003)	0.91	0.88
(402)	0.82	0.86
(006)	0.47	0.44
(502)	0.64	0.75
(106)	0.44	0.44
(206)	0.42	0.43
(107)	0.39	0.38

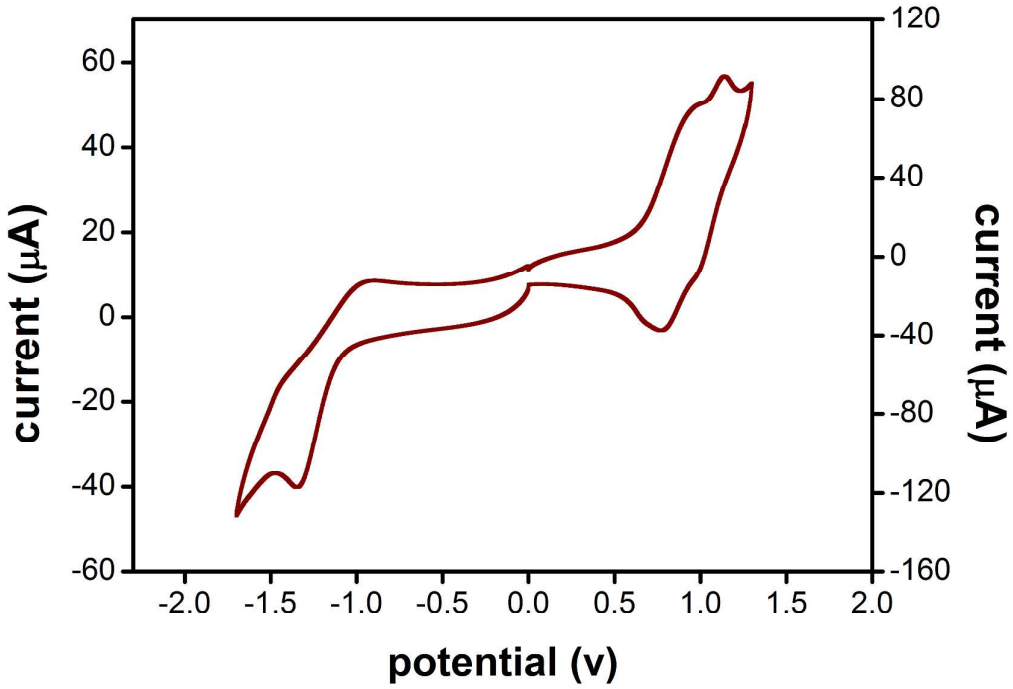

Figure S5. Cyclic voltammograms of DTS(F_2BT)$_2$ (10^{-3} M) in CH_2Cl_2 at scan rate 20 mV/s, with working and counter electrodes Pt and reference electrode Ag/AgCl; supporting electrolyte *n*-Bu_4NPF_6 (0.1 M).

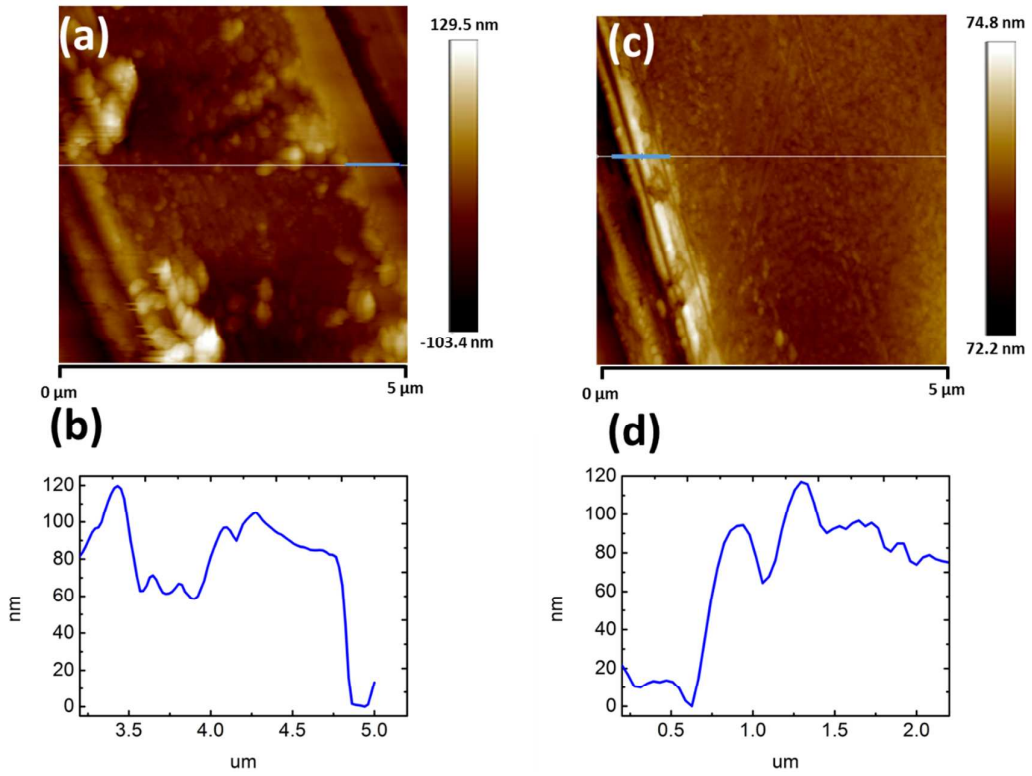

Figure S6. AFM topography and cross-section profiles of the DTS(F_2BT)$_2$:PC_{71}BM active films processed without DIO (a), (b) and with DIO (c),(d).

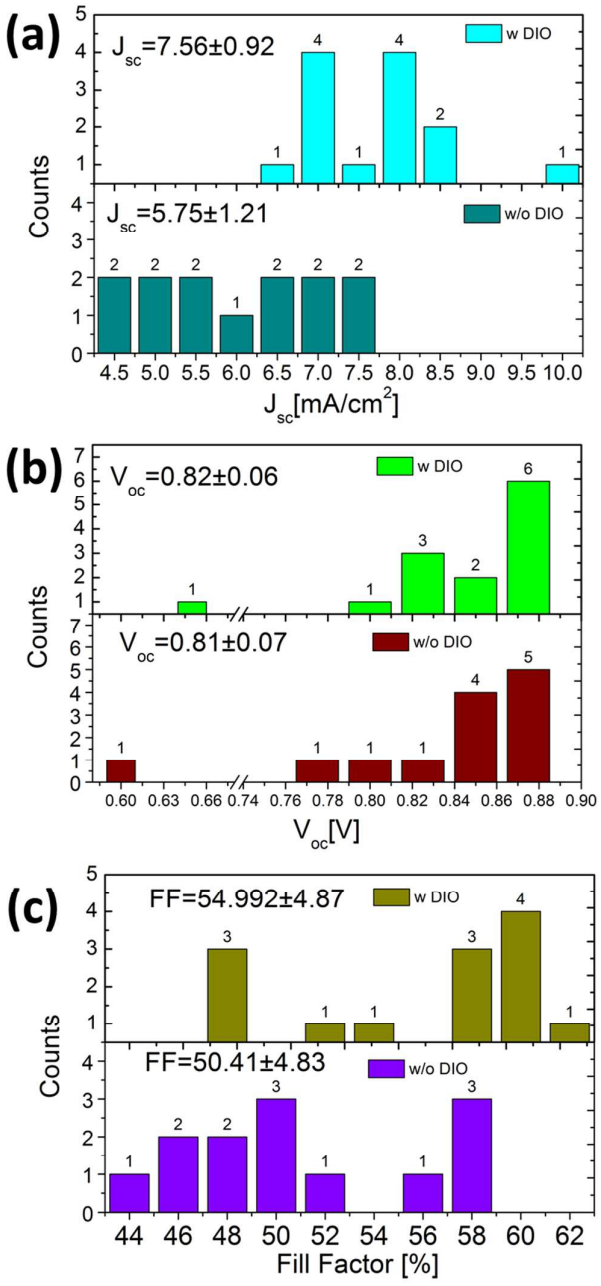

Figure S7. Histograms of (a)J_{sc}, (b)V_{oc}, and (c)Fill Factor for sets of DTS(F_2BT)$_2$–$PC_{71}BM$-based inverted BHJ PSC devices processed with and without DIO (0.4 vol %). Each sets is composed of 13 separate devices.